PHYSICAL REVIEW B **92**, 041116(R) (2015)

Possible role of bonding angle and orbital mixing in iron pnictide superconductivity: Comparative electronic structure studies of LiFeAs and Sr_2VO_3FeAs

Y. K. Kim,[1,2] Y. Y. Koh,[1] W. S. Kyung,[1] G. R. Han,[1] B. Lee,[3] Kee Hoon Kim,[3] J. M. Ok,[4] Jun Sung Kim,[4] M. Arita,[5] K. Shimada,[5] H. Namatame,[5] M. Taniguchi,[5] S.-K. Mo,[2] and C. Kim[1,*]

[1]*Institute of Physics and Applied Physics, Yonsei University, Seoul 120-749, Korea*

[2]*Advanced Light Source, Lawrence Berkeley National Laboratory, Berkeley, California 94720, USA*

[3]*CeNSCMR, Department of Physics and Astronomy, Seoul National University, Seoul 151-747, Korea*

[4]*Department of Physics, Pohang University of Science and Technology, Pohang 790-784, Korea*

[5]*Hiroshima Synchrotron Radiation Center, Hiroshima University, Higashi-Hiroshima, Hiroshima 739-0046, Japan*

(Received 12 August 2014; revised manuscript received 1 June 2015; published 27 July 2015)

A well-known universal feature among iron pnictide superconductors is the correlation between the As-Fe-As bonding angle and the superconducting transition temperature. However, the origin of such a correlation has not been clearly understood despite its potential importance in understanding the mechanism of superconductivity. Here, we present comparative electronic structure studies of LiFeAs and Sr_2VO_3FeAs, two representative systems without any dopant that can show bonding angle dependence of the electronic structure. Captured distinct features of the higher T_c compound Sr_2VO_3FeAs such as an unusual k_z modulation and anomalous polarization dependence suggest that the difference between the two systems is in the interorbital coupling strength. This could be the essential element of the bonding angle dependence that allows an enhanced pairing instability and T_c.

DOI: 10.1103/PhysRevB.92.041116 PACS number(s): 74.25.Jb, 74.62.Bf, 74.70.Xa, 79.60.−i

Despite the intensive and extensive efforts, the mechanism for the superconductivity in iron-based superconductors (IBS) is still under strong debate and no consensus has been made so far. Part of the difficulty comes from the fact that there are many variants in IBS with different physical properties. Overcoming such a difficulty requires finding universal traits of IBS compounds. A remarkable universal feature that can shed light on the superconducting mechanism in IBS is the special relationship between the As-Fe-As bonding angle and the transition temperature T_c. The maximum T_c is achieved with an optimal bonding angle that makes a $FeAs_4$ tetrahedron regular [1,2]. This fact implies an importance of the role of the bonding angle for the superconductivity in IBS. Despite the importance of the bonding angle, a microscopic understanding of how it is connected to the superconductivity is unclear yet.

One of the key elements that varies with the bonding angle is the momentum dependent electronic structure. It has been studied theoretically [3] but related experimental studies such as angle-resolved photoemission (ARPES) are lacking. LiFeAs (LFA) and Sr_2VO_3FeAs (SVOFA) are almost ideal systems to investigate the issue. LFA has a smaller bonding angle with a relatively lower T_c of 18 K [2,4] while SVOFA has a higher T_c of 37 K [1,5] with a bonding angle close to the optimal value. The fact that both systems show superconductivity without any doping [4,5] supports the notion that the bonding angle is the most dominant parameter. Therefore the difference in LFA and SVOFA electronic structures can represent the bonding angle dependence effect. Furthermore, both systems have neutral cleavage planes, which makes the two systems suitable for comparative studies of the intrinsic electronic structure by ARPES.

ARPES studies have already been performed on LFA [6,7] but SVOFA has hardly been studied, with only one report [8] due to the difficulty in growing suitable single crystals for ARPES. Recently, we succeeded in growing SVOFA single crystals for ARPES studies. In this Rapid Communication, we present a comparative electronic structure study on LFA and SVOFA using ARPES. The k_z-dependent band structure of SVOFA and its orbital character was determined. A detailed analysis reveals that the SVOFA electronic structure has orbital mixed nature and a relatively strong Fermi surface (FS) nesting instability compared to LFA. Through that, we suggest a possible role of the bonding angle in terms of the different interorbital coupling strengths.

Single-crystalline LFA was synthesized using the Sn-flux [9] and self-flux methods. SVOFA single crystals were grown using the self-flux method. ARPES measurements on LFA were performed at the beamline 9A at the Hiroshima Synchrotron Radiation Center (HiSOR), the beamline 5-4 at the Stanford Synchrotron Radiation Lightsource and the beamline 7.0.2 at the Advanced Light source (ALS). Measurements on SVOFA were performed at the beamline 10.0.1 at ALS. Samples were cleaved at 10 K. Subsequent ARPES experiments were also performed at 10 K in a vacuum better than 4×10^{-11} Torr. The polarization was controlled by using an elliptically polarized undulator at the HiSOR and by rotating the sample and analyzer at ALS.

In Fig. 1, we plot the FSs and the band dispersions of the two systems. Note that the data for LFA (SVOFA) is plotted in gold (gray) color scale throughout this Letter to avoid a possible confusion. The band dispersions along the two different Γ-X directions are plotted in Figs. 1(c)–1(f). The two equivalent Γ-X directions in these panels are distinguished and specific bands are enhanced or suppressed due to the polarization dependence (experimental geometry). Our results indicate that the overall electronic structure of both systems is similar to that of other iron pnictide systems [6,10–13]. It is noteworthy that the low-energy electronic structure of SVOFA follows the general iron pnictide band dispersion, confirming the absence of vanadium bands near the E_F as was previously reported [8].

*changyoung@yonsei.ac.kr

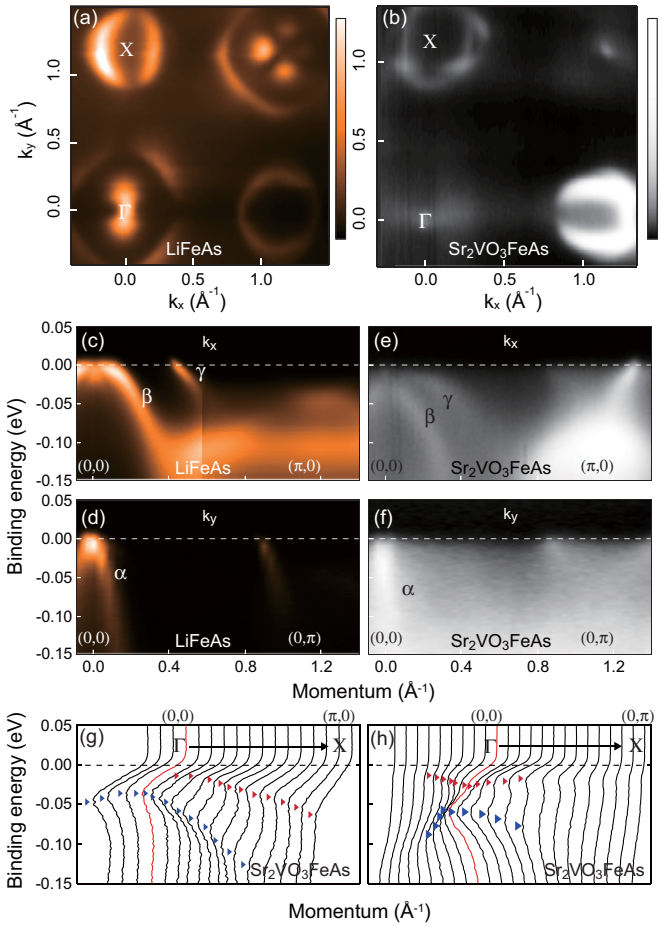

FIG. 1. (Color online) Fermi surfaces of (a) LFA and (b) SVOFA. Γ-X band dispersions of LFA along the (c) k_x and (d) k_y directions. SVOFA ARPES data along the (e) k_x and (f) k_y directions. Equivalent k_x and k_y directions are distinguished due to the polarization dependence. Stacked EDCs around the Γ point of SVOFA along the (g) k_x, (0,0)-(π,0) and (h) k_y, (0,0)-(0,π) directions.

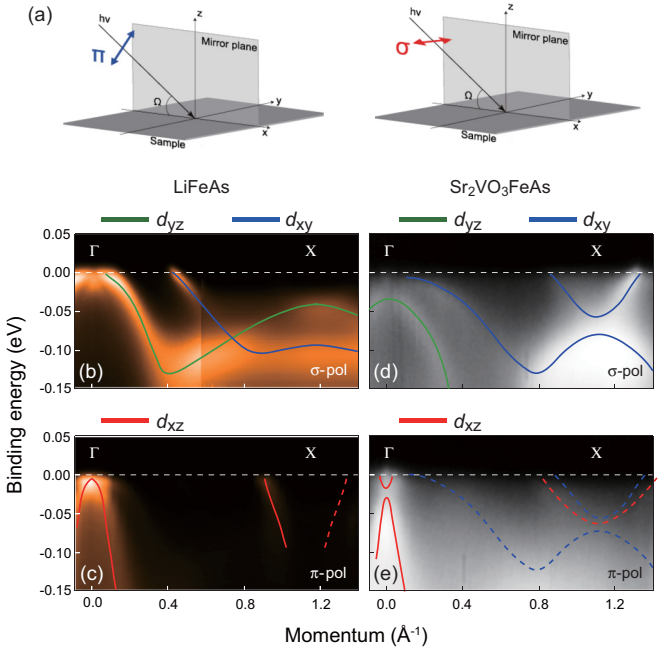

FIG. 2. (Color online) (a) Experimental geometries for polarization dependent experiments, π polarization (left) and σ polarization (right). (b) and (c) Band dispersions of LFA along Γ-X high-symmetry line with different polarization. (d) and (e) same for SVOFA. Color coded lines above panel indicate the transition allowed orbitals in each geometry with color codes of d_{xy} (blue), d_{yz} (green), and d_{xz} (red).

In comparing the results from the two systems, near E_F, the sizes of electron pockets at the zone corner in both systems are similar while the hole pocket sizes at the zone center are different. Particularly, the size of outermost γ hole pocket in LFA is much larger than that of SVOFA. For LFA, the β band, one of the inner hole bands, crosses the Fermi level while the other inner hole band α remains below E_F. Meanwhile, both α and β bands in SVOFA do not cross E_F, that is, the maxima of the hole bands at the Γ point are located right below the Fermi level. Instead, there appears an additional tiny electron band close to E_F. This electron band can be seen more clearly in the energy distribution curves (EDCs) around the Γ point as shown in Figs. 1(g) and 1(h).

In order to investigate the orbital characters of the systems in our study, we performed polarization dependent measurements as shown in Fig. 2. A schematic of the experimental geometry is illustrated in Fig. 2(a). A clear polarization dependence is seen in the data along the k_x and k_y axes [the mirror plane that includes the line of photon incidence is along the k_x direction as shown in Fig. 2(a)]. The transition-allowed orbitals in each geometry, determined by the parity as reported in previous studies [7,14–16], are shown at the top of each panel with color coded lines: red for d_{xz}, green for d_{yz}, and blue for d_{xy} orbitals [see Figs. 2(b)–2(i)]. The orbital characters of the bands can then be determined from these selection rules and the polarization dependence data.

A noticeable aspect is that the polarization dependence, especially for the hole bands, is rather weak and anomalous for SVOFA. LFA has a strong polarization dependence so that each band can be seen only in the transition allowed geometry and is invisible in the transition forbidden geometry. On the other hand, the spectral weight from the γ band survives in every geometry for SVOFA. If the γ band in SVOFA has d_{xy} orbital character as in LFA or other IBSs [7,14–16], the γ band should not appear in the geometries where the transition from the d_{xy} orbital is forbidden. The β band also shows an unusual polarization dependence, distinctly different from the cases of other iron pnictides. The band can only be seen in one geometry where a transition from the d_{xy} orbital is allowed and does not appear in the other geometries where a d_{xy} transition is forbidden.

A natural explanation of these observations is that the bands in SVOFA have a mixed orbital character, especially the hole bands. For example, the γ band is not solely from d_{xy}, but is a mixture of d_{xy}, d_{yz}, and d_{xz} (that is, $|\gamma\rangle = A|xy\rangle + a|yz/xz\rangle$). The contribution from the other orbitals, d_{xz}/d_{yz}, can produce a spectral weight in the d_{xy} forbidden geometry. In a similar manner, the α and β bands also have a d_{xy} contribution, which can explain the polarization dependence of the β band (visible only when the transition from the d_{xy} orbital is allowed).

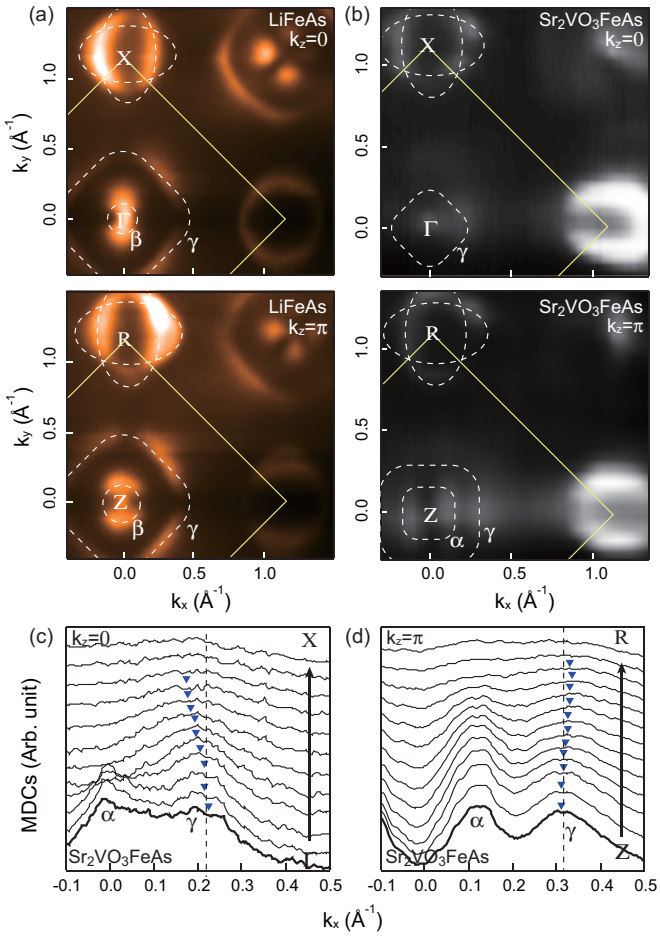

FIG. 3. (Color online) FSs of (a) LFA and (b) SVOFA at $k_z = 0$ (upper) and π (lower). FSs were determined based not only on the FS maps but also on EDCs and MDCs. Stacked MDCs of SVOFA at E_F along k_x direction taken from a constant energy map at (c) $k_z = 0$ and (d) $k_z = \pi$.

If the γ band consists of orbital mixed states and has no longer pure in-plane orbital character (d_{xy}), it must show finite k_z dispersion due to the contribution from d_{xz}/d_{yz} orbitals. This contrasts with the observation that bands with an in-plane orbital character in IBS usually do not show strong k_z dependence [17–19]. To investigate the k_z dependence in the electronic structure, photon energy dependent measurements were carried out. Results are given in Fig. 3 with FSs of the two systems measured at $k_z = 0$ and π. In the LFA case, the inner hole pocket and electron pockets show a weak k_z dependence and no k_z dependence is observed for the outer γ pocket, consistent with previous results [7]. SVOFA also mostly has a similarly weak k_z dependence. However, the γ pocket shows a strong k_z dependent modulation as expected from the mixed orbital nature. Naturally, the shape of the FS change as a function of k_z, which can be seen clearly from the stacked momentum distribution curves (MDCs) at E_F along the k_x direction (thick solid line corresponds to $k_y = 0$) [see Figs. 3(c) and 3(d)]. In the $k_z = 0$ case, k_F, indicated with blue triangles, clearly deviates from the dashed line as k_y increases, suggesting rectangular shape of FS with a corner toward to X point. In the $k_z = \pi$ case, the overall k_F trend follows the straight line in contrast to the $k_z = 0$ case, indicating a corner of rectangular FS in this case is heading to M point as shown with guide lines drawn in Fig. 3(b).

This unusual k_z dependence of the γ band in SVOFA can be fully explained by the orbital mixing effect. Due to a symmetry reason, the d_{xz}/d_{yz} orbital contribution varies as a function of k_z [dominant d_{xy} (d_{xz}/d_{yz}) weight at $k_z = 0$ (π)]. Then k_z-dependent FS shape changes can be understood in terms of the change in the orbital symmetry and correlation strength. The fact that the FS shape at $k_z = 0(\pi)$ follows the symmetry of d_{xy} (d_{xz}/d_{yz}) orbital, like in the case of Sr_2RuO_4 FS [20], clearly indicates orbital mixing and variation of orbital weight along the k_z. A little reduction of the γ pocket size at $k_z = 0$ where the band is predominantly of d_{xy} character, indicated in Figs. 3(c) and 3(d), can be understood as a result of the localized nature of the d_{xy} orbital relative to the d_{xz}/d_{yz} orbital in iron pnictides, as revealed by dynamic mean field theory calculations [21].

The band dispersions along with the orbital characters obtained from the experimental data are summarized in Fig. 4(a). The orbital characters are drawn in the same color

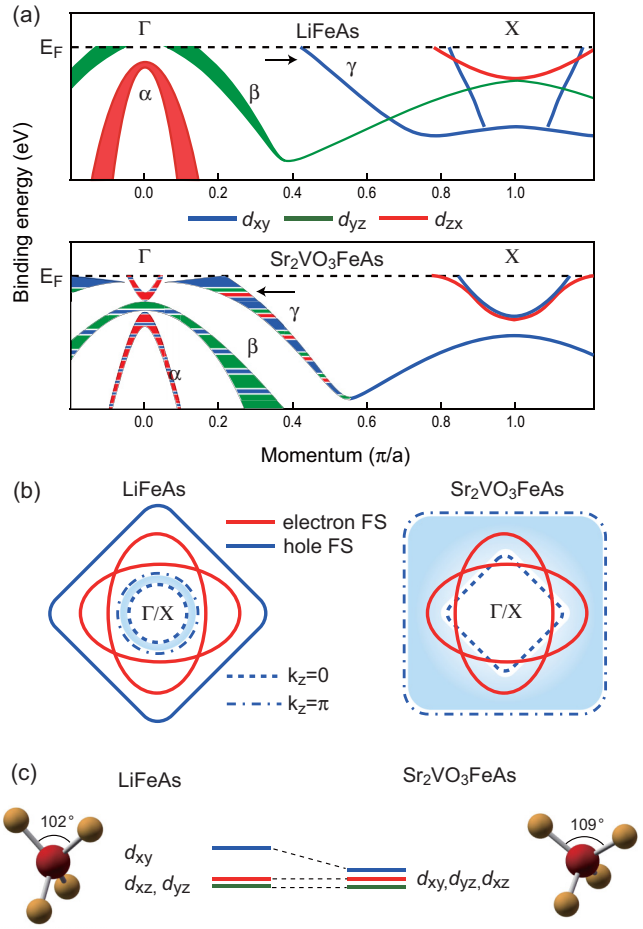

FIG. 4. (Color online) (a) Summary of orbital characters of the bands for LFA (upper) and SVOFA (lower). Widths of the lines indicate the degree of k_z dispersions. Same color codes are used as in Fig. 3. Stripe pattern means a state with mixed orbital nature. (b) Schematic of FS nesting conditions with a nesting momentum $\vec{q} = (\pi,\pi)$. The band dispersions and the size of the pockets are extracted from the experimental data. (c) Schematic of the $FeAs_4$ tetrahedron electronic structure of the two systems.

codes used in Fig. 2. The k_z dependence of each band is reflected in the linewidth. The hole bands near the Γ point show different characters between LFA and SVOFA, while the electron bands share similar characters. Of particular interest is that the γ bands in respective systems show a dramatic difference. In LFA, the γ band maximum is located at a much higher energy than E_F, while the other two band maxima (α and β) are close to E_F. Meanwhile, the band maxima of all three hole bands of SVOFA are closely located near E_F. Furthermore, as discussed before, the SVOFA γ band shows rather anomalous features: a strong k_z dependence and mixed orbital nature, distinctly different from the LFA case.

As a consequence of the band dispersions, LFA and SVOFA possess different FS nesting instability conditions. In Fig. 4(b), the hole FS is overlaid with the electron FS for the two systems to visualize the degree of the FS nesting instability. The colored areas, bounded by $k_z = 0$ and π FSs, indicate the k_z dependence of the d_{xy} hole FS. SVOFA clearly shows a stronger nesting instability than LFA, especially at $k_z = 0$ where the hole FS matches the electron FS very well for SVOFA. Meanwhile, LFA FSs show poor overlap for the entire k_z range. Note that the strong nesting instability in SVOFA does not result in magnetism since the magnetism is known to be favored by nesting between bands with the same orbital characters [21]. A nesting instability with a mixed orbital band opens an interorbital coupling channel, not an intraorbital coupling.

Thus both orbital mixing and strong nesting instability consistently point to a strong interorbital coupling instability in SVOFA, but not in LFA. Together with the fact that SVOFA has a higher T_C than LFA, the interorbital coupling instability can be regarded as an important ingredient for the superconductivity and a potential connection between the bonding angle and T_C. Our experimental results evidence the presence and possible role of the interorbital coupling instability. This aspect has been discussed only in a number of theoretical studies [22–24].

As stated in the beginning, the major difference between LFA and SVOFA is the bonding angle α. The fact that the electron and hole FS areas are approximately the same for both systems indicates no charge doping difference between the two systems, further confirming our claim that the observed difference represents the bonding angle dependence. LFA has a bonding angle of $\alpha = 102^\circ$ and the $FeAs_4$ tetrahedron is elongated. Meanwhile, the bonding angle for SVOFA is $\alpha = 109^\circ$, which is close to the optimal value and the $FeAs_4$ tetrahedron is almost regular [see Fig. 4(c)]. The three t_{2g} orbital states are thus nearly degenerate in the SVOFA case, while LFA has the d_{xy} orbital state located at a higher energy level than other orbital states [3]. This is reflected in the measured band dispersions of the two systems shown in Fig. 4(a). The degeneracy in the SVOFA electronic states induces orbital mixing and thus scattering channels for interorbital coupling which could enhance the pairing instability and T_c. We believe this gives a possible explanation for the observed correlation between the bonding angle and the transition temperature. Finally, we note that the d_{xy} orbital state takes the "steersman's" role as its level is being strongly modified upon the bonding angle change due to its localized nature compared to other orbitals [21].

This work was supported through (National Research Foundation of Korea (NRF) Grants No. 2010-0018092 and No. 2006-08658. The work at SNU was financially supported by the National Creative Research Initiative (2010-0018300) through the NRF of Korea. The work at POSTECH was supported by NRF through the Mid Career Researcher Program (Grant No. 2012-013838) and the Max Planck POSTECH/KOREA Research Initiative Program (No. 2011-0031558) and also by IBS (No. IBSR014-D1-2014-a02). The experiments at HiSOR were performed under the approval of HSRC (Proposals No. 11-A-11 and No. 12-A-23). The ALS is supported by the Office of Basic Energy Sciences, of the U.S. DOE under Contract No. DE-AC02-05CH11231.

[1] C.-H. Lee, A. Iyo, H. Eisaki, H. Kito, M. T. Fernandez-Diaz, T. Ito, K. Kihou, H. Matsuhata, M. Braden, and K. Yamada, J. Phys. Soc. Jpn. **77**, 083704 (2008).

[2] Y. Mizuguchi, Y. Hara, K. Deguchi, S. Tsuda, T. Yamaguchi, K. Takeda, H. Kotegawa, H. Tou, and Y. Takano, Supercond. Sci. Technol. **23**, 054013 (2010).

[3] Hidetomo Usui and Kazuhiko Kuroki, Phys. Rev. B **84**, 024505 (2011).

[4] J. H. Tapp, Z. Tang, B. Lv, K. Sasmal, B. Lorenz, P. C. W. Chu, and A. M. Guloy, Phys. Rev. B **78**, 060505(R) (2008).

[5] X. Zhu, F. Han, G. Mu, P. Cheng, B. Shen, B. Zeng, and H.-H. Wen, Phys. Rev. B **79**, 220512(R) (2009).

[6] S. V. Borisenko, V. B. Zabolotnyy, D. V. Evtushinsky, T. K. Kim, I. V. Morozov, A. N. Yaresko, A. A. Kordyuk, G. Behr, A. Vasiliev, R. Follath, and B. Bűchner, Phys. Rev. Lett. **105**, 067002 (2010).

[7] T. Hajiri, T. Ito, R. Niwa, M. Matsunami, B. H. Min, Y. S. Kwon, and S. Kimura, Phys. Rev. B **85**, 094509 (2012).

[8] T. Qian, N. Xu, Y.-B. Shi, K. Nakayama, P. Richard, T. Kawahara, T. Sato, T. Takahashi, M. Neupane, Y.-M. Xu, X.-P. Wang, G. Xu, X. Dai, Z. Fang, P. Cheng, H.-H. Wen, and H. Ding, Phys. Rev. B **83**, 140513(R) (2011).

[9] B. Lee, S. Khim, J. S. Kim, G. R. Stewart, and K. H. Kim, Europhys. Lett. **91**, 67002 (2010).

[10] M. Yi, D. H. Lu, J. G. Analytis, J.-H. Chu, S.-K. Mo, R.-H. He, M. Hashimoto, R. G. Moore, I. I. Mazin, D. J. Singh, Z. Hussain, I. R. Fisher, and Z.-X. Shen, Phys. Rev. B **80**, 174510 (2009).

[11] C. Liu, T. Kondo, N. Ni, A. D. Palczewski, A. Bostwick, G. D. Samolyuk, R. Khasanov, M. Shi, E. Rotenberg, S. L. Bud'ko, P. C. Canfield, and A. Kaminski, Phys. Rev. Lett. **102**, 167004 (2009).

[12] L. X. Yang, Y. Zhang, H. W. Ou, J. F. Zhao, D. W. Shen, B. Zhou, J. Wei, F. Chen, M. Xu, C. He, Y. Chen, Z. D. Wang, X. F. Wang, T. Wu, G. Wu, X. H. Chen, M. Arita, K. Shimada, M. Taniguchi, Z. Y. Lu, T. Xiang, and D. L. Feng, Phys. Rev. Lett. **102**, 107002 (2009).

[13] M. Yi, D. Lu, J.-H. Chu, J. G. Analytis, A. P. Sorini, A. F. Kemper, B. Moritz, S.-K. Mo, R. G. Moore, M. Hashimoto, W.-S. Lee, Z. Hussain, T. P. Devereaux, I. R. Fisher, and Z.-X. Shen, Proc. Natl. Acad. Sci. USA **108**, 6878 (2011).

[14] Y. Zhang, F. Chen, C. He, B. Zhou, B. P. Xie, C. Fang, W. F. Tsai, X. H. Chen, H. Hayashi, J. Jiang, H. Iwasawa, K. Shimada, H. Namatame, M. Taniguchi, J. P. Hu, and D. L. Feng, Phys. Rev. B **83**, 054510 (2011).

[15] Y. Zhang, C. He, Z. R. Ye, J. Jiang, F. Chen, M. Xu, Q. Q. Ge, B. P. Xie, J. Wei, M. Aeschlimann, X. Y. Cui, M. Shi, J. P. Hu, and D. L. Feng, Phys. Rev. B **85**, 085121 (2012).

[16] X.-P. Wang, P. Richard, Y.-B. Huang, H. Miao, L. Cevey, N. Xu, Y.-J. Sun, T. Qian, Y.-M. Xu, M. Shi, J.-P. Hu, X. Dai, and H. Ding, Phys. Rev. B **85**, 214518 (2012).

[17] Z. R. Ye, Y. Zhang, F. Chen, M. Xu, Q. Q. Ge, J. Jiang, B. P. Xie, and D. L. Feng, Phys. Rev. B **86**, 035136 (2012).

[18] Y. Zhang, L. X. Yang, F. Chen, B. Zhou, X. F. Wang, X. H. Chen, M. Arita, K. Shimada, H. Namatame, M. Taniguchi, J. P. Hu, B. P. Xie, and D. L. Feng, Phys. Rev. Lett. **105**, 117003 (2010).

[19] T. Yoshida, I. Nishi, S. Ideta, A. Fujimori, M. Kubota, K. Ono, S. Kasahara, T. Shibauchi, T. Terashima, Y. Matsuda, H. Ikeda, and R. Arita, Phys. Rev. Lett. **106**, 117001 (2011).

[20] A. Damascelli, D. H. Lu, K. M. Shen, N. P. Armitage, F. Ronning, D. L. Feng, C. Kim, Z.-X. Shen, T. Kimura, Y. Tokura, Z. Q. Mao, and Y. Maeno, Phys. Rev. Lett. **85**, 5194 (2000).

[21] G. Lee, H. S. Ji, Y. K. Kim, C. Kim, K. Haule, G. Kotliar, B. Lee, S. Khim, K. H. Kim, K. S. Kim, K.-S. Kim, and J. H. Shim, Phys. Rev. Lett. **109**, 177001 (2012).

[22] J. Zhang, R. Sknepnek, R. M. Fernandes, and J. Schmalian, Phys. Rev. B **79**, 220502(R) (2009).

[23] T. D. Stanescu, V. Galitski, and S. Das Sarma, Phys. Rev. B **78**, 195114 (2008).

[24] H. Kontani and S. Onari, Phys. Rev. Lett. **104**, 157001 (2010).